



Published in final edited form as:

Biomaterials. 2016 February ; 80: 68–79. doi:10.1016/j.biomaterials.2015.11.051.

Low cost delivery of proteins bioencapsulated in plant cells to human non-immune or immune modulatory cells

Yuhong Xiao^{1,#}, Kwang-Chul Kwon^{1,#}, Brad E. Hoffman^{2,#}, Aditya Kamesh¹, Noah T. Jones², Roland W. Herzog², and Henry Daniell^{1,*}

¹Department of Biochemistry, School of Dental Medicine, University of Pennsylvania, Philadelphia, PA

²Department of Pediatrics, College of Medicine, University of Florida, Gainesville, FL

Abstract

Targeted oral delivery of GFP fused with a GM1 receptor binding protein (CTB) or human cell penetrating peptide (PTD) or dendritic cell peptide (DCpep) was investigated. Presence of GFP⁺ intact plant cells between villi of ileum confirm their protection in the digestive system from acids/enzymes. Efficient delivery of GFP to gut-epithelial cells by PTD or CTB and to M cells by all these fusion tags confirm uptake of GFP in the small intestine. PTD fusion delivered GFP more efficiently to most tissues or organs than other two tags. GFP was efficiently delivered to the liver by all fusion tags, likely through the gut-liver axis. In confocal imaging studies of human cell lines using purified GFP fused with different tags, GFP signal of DCpep-GFP was only detected within dendritic cells. PTD-GFP was only detected within kidney or pancreatic cells but not in immune modulatory cells (macrophages, dendritic, T, B, or mast cells). In contrast, CTB-GFP was detected in all tested cell types, confirming ubiquitous presence of GM1 receptors. Such low-cost oral delivery of protein drugs to sera, immune system or non-immune cells should dramatically lower their cost by elimination of prohibitively expensive fermentation, protein purification cold storage/transportation and increase patient compliance.

Keywords

Chloroplasts; cell-penetrating peptides; molecular farming; protein drug delivery

*Correspondence: Henry Daniell, Ph.D, Professor and Director of Translational Research, University of Pennsylvania, Philadelphia, hdaniell@upenn.edu, Tel: 215-746-2563.

#authors made equal contributions to this study.

Author contributions

HD conceived and supervised the study and designed experiments. RWH offered guidance on mice studies and interpreted data. YX, KCK, AK (Aditya Kamesh), RWH and HD wrote this manuscript. KCK contributed data and text on Fig. 1 and Fig. 4 except for 4C; YX contributed data in Table 1, Fig. 2 and Fig. 5 except for mast cell. AK (Aditya Kamesh) contributed data for Fig 4C and wrote associated text. BEH and NTJ contributed data in figure 3.

Publisher's Disclaimer: This is a PDF file of an unedited manuscript that has been accepted for publication. As a service to our customers we are providing this early version of the manuscript. The manuscript will undergo copyediting, typesetting, and review of the resulting proof before it is published in its final citable form. Please note that during the production process errors may be discovered which could affect the content, and all legal disclaimers that apply to the journal pertain.

1. Introduction

Biopharmaceuticals produced in current systems are prohibitively expensive and are not affordable for a large majority of the global population. In the US, the average annual cost of protein drugs is 25-fold higher than for small molecule drugs. The cost of protein drugs (\$140 billion in 2013) exceeds the GDP of >75% of countries around the globe, making them unaffordable in these countries [1]. One third of the global population earning <\$2 per day cannot afford any protein drugs. Although recombinant insulin has been sold commercially for five decades, it is still not affordable for a large majority of global population. This is because of their production in prohibitively expensive fermenters, coupled with a need for purification, cold storage/transportation, sterile delivery, and short shelf life. Oral delivery of protein drugs has been elusive for decades because of their degradation in the digestive system and inability to cross the gut epithelium for delivery to target cells.

However, several recent studies have indirectly shown that plant cell wall protects expressed protein drugs from acids and enzymes in the stomach via bio-encapsulation [2, 3]. Human digestive enzymes are incapable of breaking down glycosidic bonds in carbohydrates that make up plant cell wall. However, when intact plant cells containing protein drugs reach the gut, commensal microbes could digest plant cell wall and release protein drugs in the gut lumen. Bacteria inhabiting the human gut have evolved to utilize complex carbohydrates in plant cell wall and are capable of utilizing almost all plant glycans [4, 5]. Fusion of the (nontoxic) Cholera toxin B subunit (CTB) to green fluorescent protein (GFP) expressed in chloroplasts and bioencapsulated in plant cells was delivered across the gut epithelium through GM1 receptors and GFP was released into the circulatory system [6]. Fusion of CTB to therapeutic proteins facilitates their effective oral delivery for induction of oral tolerance [7–11] or functional proteins to sera [12–14] or even across blood brain or retinal barriers [15, 16].

Foreign proteins can also be delivered into living cells by fusion with protein transduction domains (PTDs) with cell membrane penetration properties that do not require specific receptors [17]. The peptide and protein transduction domains (PTDs) are small cationic peptides containing 8–16 amino acids in length, and most frequently function as transporter for delivery of macromolecules [17]. PTDs carry molecules into cells by a receptor independent, fluid-phase macro-pinocytosis, which is a special form of endocytosis. Although different PTDs show similar characteristics of cellular uptake, they vary in their efficacy for transporting protein molecules into cells. The efficacy for cellular uptake has been found to correlate strongly with the number of basic amino acid residues. Since PTDs have been shown to deliver biologically active proteins in cultured mammalian cells and in animal model *in vivo* and *in vitro* [18–20], the PTD fused protein delivery method should have great therapeutic drug delivery potential.

T and B lymphocytes are major cellular components of the adaptive immune response, but their activation and homeostasis are controlled by dendritic cells. B cells can recognize native Ag directly through B cell receptor on their surface and secrete antibodies. However, T cells are only able to recognize peptides that are displayed by MHC class I and II

molecules on the surface of APCs. Macrophage is one type of professional antigen-presenting cells, having many important roles including removal of dead cells and cell debris in chronic inflammation and initiating an immune response [21,22]. Macrophages participate in the orchestration of primary and secondary immune responses. Mast cells are involved in generating the first inflammatory response during infection, which is important for initiating innate and adaptive immunity. When activated, a mast cell rapidly releases its characteristic granules and various hormonal mediators into the interstitium. Therefore, mast cells play important roles in wound healing, allergic disease, anaphylaxis and autoimmunity.

Dendritic cell is one of the most important immune modulatory cells. Dendritic cell forms a complex with multifunctional APCs and play critical roles in anti-pathogen activities. Moreover, dendritic cells differentiate into different type of functional cells, stimulated by different antigens and induce humoral or cellular immunity. Conversely, DCs are also critical for the homeostasis of regulatory T cells (Treg), extrathymic induction of Treg, and for immune tolerance induction in transplantation and treatment of allergy or autoimmune disease. The tissue microenvironment, activation signals, and subsets of DCs are important parameters that determine whether antigen presentation by DCs result in immunity or tolerance [23–25]. Therefore, targeted *in vivo* delivery of antigens to DCs may not only be useful for inducing tumor-specific immune responses and establish novel strategies for vaccine development, cancer immunotherapy, but also for tolerance induction protocols [26–28]. For example, the gut associated lymphatic tissues (GALT) provide the largest surface area for antigen entry into the body and a very unique microenvironment with tolerogenic properties, including expression of the immune suppressive cytokines IL-10 and TGF- β [29–31]. Gut epithelial cells and CX1CR5⁺ macrophages sample antigens from the gut lumen. In particular in the endothelium of Peyer's patches, microfold cells (M cells) endocytose and phagocytose antigens to channel these to DCs. CD11c⁺ DCs in the gut contain a high proportion of CD103⁺ DC, which express TGF- β preferentially induce Treg [32]. Recently, we demonstrated that oral tolerance induction to coagulation factors in hemophilic mice upon delivery of bioencapsulated CTB-fusion antigens was associated with increased CD103⁺ DC frequency, antigen uptake by CD103⁺ DC, and induction of several subsets of Treg [9, 10]. Also increased were plasmacytoid DC, which also have important immune modulatory functions [33]. Recently, DC peptide (DCpep) has been developed as a ligand to mucosal DCs [26]. This small peptide binds to a DC-specific receptor and facilitates transportation of macromolecules into DC. These properties can be exploited to efficiently deliver various molecules to DCs for antigen presentation, to block their maturation, or to modulate their functions.

In this study, we investigate oral administration of plant cells expressing GFP fused with different tags in chloroplasts and evaluate cellular targeting and their bio-distribution. Delivery of PTD, DCpep, and CTB fusions across the gut epithelium utilizing distinct pathways result in systemic delivery, bio-distribution, and, perhaps most importantly, distinct patterns of uptake by non-immune or immune modulatory cells. These peptides could be used to deliver therapeutic proteins to sera, immune modulatory cells or specific tissues.

2. Methods

2.1. Creation of transplastomic lines expressing different tagged GFP fusion proteins

The transplastomic plants expressing CTB-GFP and PTD-GFP were created as described in previous studies [6, 34]. DC specific peptide, identified from screening of the Ph.D. 12-mer phage display library [26] was conjugated to the C-terminus of GFP and cloned into chloroplast transformation vector and transplastomic lines expressing DCpep-GFP were created and homoplasmic lines were confirmed using Southern blot assay as described previously [35]. Also, expression of GFP tagged proteins were confirmed by visualizing green fluorescence from the leaves of each construct under UV illumination.

2.2. Lyophilization

The harvested mature leaves were stored at -80°C and freeze-dried using lyophilizer (Genesis 35XL, VirTis SP Scientific) by which frozen and crumbled small pieces of leaves are subject to sublimation under the condition of vacuum (400 mTorr) and gradual augmentation of chamber temperature from -40°C to 25°C for 3 days. The lyophilized leaves were then ground in a coffee grinder (Hamilton Beach) at maximum speed 3 times (10 sec each). The powdered plant cells were stored under air-tight and moisture-free condition at room temperature with silica gel.

2.3. Quantification of GFP fusion proteins and GM1 binding assay

The densitometry assay for quantification of GFP fusion proteins and GM1 ELISA assay were carried out according to previous method [14] except for using GFP standard protein (Vector laboratories MB-0752-100) and mouse monoclonal anti-GFP antibody (EMD MILLIPORE MAB3580). Non-denaturing Tris-tricine gel for identification of pentameric structure of CTB-GFP was performed according to previous study [36].

2.4. Purification of tag-fused GFP proteins

The protein purification of GFP fused peptides, PTD-GFP and DCpep-GFP, was performed by organic extraction/FPLC based method as described before [37]. Approximately 200 mg lyophilized plant cells were homogenized in 10 ml of plant extraction buffer (100 mM NaCl, 10 mM EDTA, 200 mM Tris-Cl pH 8.0, 0.2% TritonX, 400 mM Sucrose, 2% v/v PMSF, 1 protease inhibitor tablet in 10 ml total volume). The homogenate was spun down after sonication and the supernatant was collected. The supernatant was transferred to a 50 ml falcon tube and subjected to organic extraction as performed previously [37]. The plant extract was treated with saturated ammonium sulfate to a final concentration of 70% in the extract. Then $\frac{1}{4}$ th of the total extract volume of 100% ethanol was added, mixed vigorously for 2 min and then spun down. The resulting organic phase (upper phase) was collected to a fresh 50 ml falcon tube. To the remaining aqueous phase, $\frac{1}{16}$ th of total volume of 100% ethanol was added, shaken vigorously for 2 min and then spun down again. The organic phases from both the spins were pooled together and $\frac{1}{3}$ rd of total volume of 5 M NaCl and $\frac{1}{4}$ th of the resulting volume of n-butanol was added and shaken vigorously for 2 min and spun down. The resulting organic extract layer (lower phase) at the bottom of the tube was collected and then desalted by running it through a 7KDa MWCO desalting column

(Thermo scientific zeba spin column 89893). The organic extract was loaded onto the desalting column and spun down as per manufacturer's instructions. Then the desalted organic extract (approximately 5ml volume) was then loaded onto a FPLC column (LKB-FPLC purification system, Pharmacia; 48mL column volume). During the purification process, the sample was washed with 3.5 column volumes of Buffer A (10mM Tris HCl, 10mM EDTA and 291gm ammonium sulfate set at pH 7.8) with 20% ammonium sulfate saturation. The column was then subjected to step wise increase in Buffer B (10 mM Tris HCl, 10 mM EDTA sulfate set at pH 7.8) to elute the GFP fusion. The protein was detected by measurement of absorbance at 280 nm, which corresponded to a single peak that was plotted on a recorder. The fraction corresponding with the peak was collected in a single tube having a total volume of 9 ml. The purified fraction was then dialyzed in 2 L of 0.01X PBS thrice and then lyophilized (Labconco lyophilizer). The lyophilized purified GFP fusions were then quantified by western blot/densitometric method.

For the purification of CTB-GFP, lyophilized leaf materials (400 mg) were resuspended in 20 ml of extraction buffer (50 mM Na-P, pH7.8; 300 mM NaCl; 0.1% Tween-20; 1 tb of EDTA-free protease inhibitor cocktail). The resuspension was sonicated and then centrifuged at 10,000 rpm for 10 min at 4°C. The supernatant was combined with 1 ml of His60 Ni resin (Clonetech, 635657), and purification was performed according to manufacturer's instructions.

2.5. Purity measurement and Coomassie staining

Total protein of purified from each GFP tag fraction was quantified using Bradford assay then as described in quantification section, densitometry assay was carried out to quantify the amount of GFP fusion protein in the fractions. Then the purity was evaluated by calculating the percentage of the amount of GFP fusion proteins to the total amount of protein obtained from Bradford assay. A non-denaturing SDS-PAGE was also performed in order to check fluorescence of the GFP fused proteins by running through a 10% SDS gel under non-denaturing conditions.

2.6. Evaluation of GFP expression

GFP presence in sera and tissues were quantified by our in house GFP ELISA. As our previously described [6, 16], the blood and tissue samples were collected at 2 and 5 hours after the last oral gavage and serum were stored at -80°C. Tissues were homogenized in RIPA buffer and supernatants were collected for GFP ELISA assay. Our in house ELISA protocol was established and the standards were calibrated based on GFP ELISA kit (AKR121; Cell Biolab). Briefly, 96-well Maxisorp plates (Nunc) were coated overnight at 4°C with goat polyclonal GFP antibody (2.5 mg/ml, Rockland) in coating buffer (PH 9.6). The plates were blocked in PBS with 3% BSA for 2hrs at 37°C. Serial 2-fold dilutions of sera in PBS with 1% BSA were added in duplicate and incubated overnight at 4°C. The plate was then incubated with biotin-conjugated rabbit polyclonal anti-GFP 1:5000 (Rockland) overnight at 4°C, followed by addition of 1:2000 diluted streptavidin peroxidases (Rockland). After further incubation for 1hr at 37°C, plates were washed and substrate solution was added and incubated for 10 min at RT. The reaction was stopped by adding 100

μ l of 2N sulfuric acid per well, and absorbance was measured using an ELISA reader at 450 nm. The results are shown as average \pm SEM.

2.7. Mice and oral delivery experiments

Eight-week-old female C57BL/6 mice (Jackson Laboratories, Bar Harbor, MI) were randomly divided into four groups (n=6 per group) and orally gavaged with each lyophilized bioencapsulated CTB-GFP, PTD-GFP and DCpep-GFP plant cells, 20 mg/per mouse/day for 3 consecutive days. All lyophilized materials were suspended in 200 μ l PBS. On the 3rd day, blood samples were collected 2 and 5 hrs after the last oral gavage. At the 5 hr time point, all mice were sacrificed, and organs (liver, kidney, lung, brain, tibialis anterior muscle) were harvested and stored at -80°C . A control group (n=6) was fed with untransformed lyophilized plant cells. Mice were housed in the animal facility of University of Florida and University of Pennsylvania under controlled humidity and temperature conditions, and the experiments were performed in accordance with the guidelines of Institutional Animal Care and Use Committees.

2.8. Immunofluorescent staining

As our previously described [8, 16], C57BL/6 mice were orally fed with GFP expressing plant cells twice by 2 hr interval. Two hours after last feeding, mice were sacrificed, live and intestines were removed. The intestine cut open longitudinally and washed by PBS, then rolled up and fixed overnight in 4% paraformaldehyde at 4°C . Liver tissue was also fixed similarly. Subsequently, fixed tissues were further incubated in 30% sucrose in PBS at 4°C and embedded in OCT. Serial sections were cut to a thickness of $10\mu\text{m}$.

For analysis of GFP expression, sections were permeabilized with 0.1% Triton X-100, and blocked with 5% donkey serum in PBS for 30 min, followed by incubation with rabbit anti-GFP antibody at 1:1000 (ab290, Abcam,) overnight at 4°C . The sections were then incubated for 30 min with Alexa Fluor 488 Donkey Anti-Rabbit IgG (Jackson ImmunoResearch) or with rhodamine-labeled Ulex europaeus agglutinin (UEA-1; Vector Labs; $10\mu\text{g}/\text{mL}$) for 10 min before being washed and mounted with or without DAPI (4, 6 diamidino-2-phenylindole). Images were captured using a Nikon Eclipse 80i fluorescence microscope and Retiga 2000R digital camera (QImaging) and analyzed with Nikon Elements software.

2.9. Uptake of purified tag-fused GFP proteins by human cell lines

To determine uptake of three tags, CTB, PTD and DC peptide in immune modulatory cells, mature dendritic cell, human T cell (Jurkat cell), human B cell (BCBL1), macrophage cells (m \emptyset), mast cells and non-immune modulatory cells, human kidney cells (293T), human pancreatic epithelioid carcinoma cells (PANC-1) and human pancreatic ductal epithelial cells (HPDE), were cultured and used for *in vitro* transformation of purified tag-fused proteins. Cells (2×10^4) were incubated in 100 μ l PBS supplemented 1% FBS combined with purified CTB (8.8 μg), PTD (13.5 μg) and DCpep (1.3 μg) fused protein, respectively, incubated at 37°C for 1 hour. After PBS washing, cell pellets were stained with 1:3000 diluted DAPI and fixed with 2% paraformaldehyde at RT for 10 min. Cells were then sealed on the slides with cyto seal and examined by confocal microscopy. For live image study,

after incubation with purified GFP fused proteins, dendritic cells were loaded on glass bottom microwell dishes (MatTek) and observed under confocal microscopy followed by nuclei staining with DAPI. For 293T, PANC-1 and macrophage cells, cells were cultured in 8 well chamber slides (Nunc) at 37°C for overnight, followed by incubation with purified CTB-GFP, PTD-GFP and DCpep-GFP (same as above) at 37°C for 1 hour. After washing wells with PBS, cells were stained with 1:3000 DAPI and fixed with 2% paraformaldehyde at RT for 10 min. For negative controls groups, cells incubated with commercial GFP (2 µg) in PBS with 1%FBS or had no treatment. After 1h of incubation, cells were washed once with PBS. Live non-fixed cells were imaged using confocal microscope.

To determine the uptake efficiency of purified GFP fusion proteins in different human cell lines, the number of cells showing GFP signals was counted and represented as percentage of over total number of cells observed. A total of 15–20 images were recorded for each cell line in three independent samples the under confocal microscope at 100x magnification.

3. Results

3.1. Creation and characterization of transplasmic lines

In this study we utilize three distinct transmucosal carriers. Interaction of CTB pentamer to GM1 receptor has been well studied as shown in the Fig. 1A. The penta-saccharide structure of GM1 receptor interacts with amino acids of CTB via hydrogen bonds [38]. In contrast, mechanisms of structures shown for PTD (Fig. 1A) or DCpep (Fig. 1A) has not been fully investigated. Secondary structures of cell-penetrating peptides (CPP) have been studied by circular dichroism (CD). Such peptides interact with negatively charged phospholipid vesicles leading to induction of secondary structures. Small uni-lamellar vesicles (SUVs) are used in such studies. However, the exact role of any secondary structure of CPPs in relation to translocation process is difficult to define. It has been shown that CPPs change their structure from alpha helix to beta sheets depending upon experimental conditions, even in simple model systems. So, they are described as “chameleons” in changing their structure, rapidly adapting to membrane environment (39). Therefore, secondary structures were not investigated in our studies but we used iterative threading assembly refinement program (I-TASSER) to predict computational 3-D structures [40]. In the Fig. 1A, the representative models were chosen based on the calculation of parameters such as confidence score (C-score), high-resolution models with root mean square deviation (RMSD) value, and template modeling score (TM-score). For example, if the TM-score, assessing topological similarity of first I-TASSER model to corresponding structure in Protein Data Bank (PDB) library, is greater than 0.5, the predicted topology is correct [40]. From the predicted model, TM-score of PTD was 0.60 ± 0.14 and that of DCpep was 0.58 ± 0.14 . In predicted structures, while PTD has helical structure, DCpep shows a loop structure. As expected, there is no similarity between the two peptides.

All three tags were fused to the green fluorescent protein (smGFP) to evaluate their efficiency and specificity. CTB was fused with GFP at the N-terminus via furin cleavage site, Pro-Arg-Ala-Arg-Arg [6]. Sixteen amino acid (RHKIWFQNRMMKWKK) derived from pancreatic and duodenal homeobox factor-1 (PDX-1) [41] is fused at the N-terminus with GFP and is referred to as PTD-GFP in this study. For nuclear targeting, additional

localization signals are required. Six amino acids (RH, RR, and KK) of the 16 aa-PTD are critical for nuclear localization of PDX-1(42). Human dendritic cell specific peptide ligand (FYPSYHSTPQRP) identified from screening of 12-mer phage display library [26] is fused to the C-terminus of GFP. Both PTD and DC-Peptide were engineered without the furin cleavage site to study entry as well as tissue distribution. All these three fusion constructs were cloned into the chloroplast transformation vectors (pLD) which were used to transform chloroplasts as described in the material methods section.

To create plants expressing GFP fusion proteins, tobacco chloroplasts were transformed using biolistic particle delivery system. As seen in the Fig. 1B, each tag-fused GFP is driven by identical regulatory sequences - the *psbA* promoter and 5' UTR regulated by light and the transcribed mRNA is stabilized by 3' *psbA* UTR. The *psbA* gene is the most highly expressed chloroplast gene and therefore *psbA* regulatory sequences are used for transgene expression in our lab [7, 35]. To facilitate the integration of the expression cassette into chloroplast genome, two flanking sequences, isoleucyl-tRNA synthetase (*trnI*) and alanyl-tRNA synthetase (*trnA*) genes, flank the expression cassette, which are identical to the native chloroplast genome sequence. The emerging shoots from selection medium were investigated for specific integration of the transgene cassette at the *trnI* and *trnA* spacer region and then transformation of all chloroplast genomes in each plant cell (absence of untransformed wild type chloroplast genomes) by Southern blot analysis with the Dig-labeled probe containing the *trnI* and *trnA* flanking sequences (Fig. 1C). As seen in Fig. 1C, *HindIII*-digested gDNAs from three lines of each GFP plant showed transformed large DNA fragments at 7.06, 6.79 and 6.78 kbp, for CTB-GFP, PTD-GFP and DCpep-GFP, respectively, when hybridized with the probe and absence of the untransformed smaller fragment (4.37 kbp). Thus, stable integration of three different GFP expression cassettes and homoplasmy of chloroplast genome with transgenes were confirmed. In addition, by visualizing the green fluorescence under UV light, GFP expression of was phenotypically monitored (Fig. 1D).

To scale up the biomass of each GFP tagged plant leaf material, each homoplasmic line was grown in a temperature- and humidity-controlled automated Daniell lab greenhouse. Fully grown mature leaves were harvested in late evenings to maximize the accumulation of GFP fusion proteins driven by light-regulated control sequences. To further increase the content of the fusion proteins on a dry weight basis, frozen leaves were freeze-dried at -40°C under vacuum. In addition to the concentration effect of proteins, lyophilization increased shelf life of therapeutic proteins expressed in plants more than one year at room temperature [13]. Therefore, in this study, lyophilized and powdered plant cells expressing GFP-fused tag proteins were used for oral delivery to mice. Immunoblot assay for the GFP fused tag proteins showed identical size proteins in fresh and 4-month old lyophilized leaves (Fig. 1E), confirming stability of fusion proteins during lyophilization and prolonged storage at room temperature. In the immunoblot image, in addition to monomers of 39.5 kDa, 29.2 kDa, and 28.3 kDa for CTB-GFP, PTD-GFP, and DCpep-GFP, respectively, dimers were also detected for PTD-GFP (58.4 kDa) and DCpep-GFP (56.6 kDa) (Fig. 1E). Homodimerization is one of GFP physio-chemical features, which occurs in solution and in crystals. The contacts between the monomers are very tight due to extensive interactions

which are composed of a core of hydrophobic side chains from each monomer and a number of hydrophilic contacts [43]. Also, CTB monomer can be self-assembled to pentameric structure which is very stable and resistant heat and denaturants due to the intersubunit interactions within pentameric structure, which is mediated by hydrogen bonds, salt bridges and hydrophobic interactions [44].

GFP protein concentration in powdered lyophilized leaf materials was 5.6 µg/mg, 24.1 µg/mg and 2.16 µg/mg for CTB-GFP, PTD-GFP, and DCpep-GFP, respectively (Fig. 1C). GFP protein concentration after lyophilization increased 17.1-, 12.7-, and 18.8-fold for CTB-GFP, PTD-GFP, and DCpep-GFP, respectively (Fig. 1F). Removal of water from fresh leaves by lyophilization is attributed to the reduction of weight by 90–95%. This effect is then manifested as 10–20 fold increase of protein per gram of dry leaves [13, 15, 45].

3.2. GFP uptake in different tissues after oral delivery of plant cells

For oral delivery, lyophilized plant cells (20 mg) were rehydrated in uniform volume (200 µl) and similar durations. Dispersed plant cells do not vary in their size because mature plant cells are uniform in size. As seen in Fig. 2, the bio-distribution of GFP does not show any significant variations. After oral delivery of lyophilized plant cells expressing GFP (fused with PTD or CTB or DC peptide), systemic GFP levels were higher in PTD-GFP fed animals than any other tags tested (Fig. 2A). Biodistribution to liver and lung was substantially higher than other tissues (skeletal muscle, kidney). GFP levels in these tissues were consistently highest for PTD fusion protein (Fig. 2B). Immunohistochemical studies using GFP-specific antibody offered further insight into the route of delivery. As shown in Fig. 3A (3C insert), sensitive method of detection of GFP using Alexa Flour 488 labeled secondary antibody revealed that the PTD tag directed some GFP uptake by gut epithelial cells. No GFP was detected when no primary antibody was used or when tissues from mice fed with untransformed tobacco cells (Fig. 3B). In order to more readily find areas of gut where plant cells are located and antigen uptake may be observed, the small intestine was rolled up prior to fixation, so that proximal and distal portions were visible on the same slide (Fig. 3C). Presence of plant cells expressing GFP in between villi of ileum (Fig. 3C and E) offers first direct proof for protection of plant cells from the digestive system. More widespread delivery of GFP to epithelial cells was also seen when using the CTB tag (Fig. 3D) and this is due to efficient targeting of the GM1 receptor with by CTB pentamers. In addition to delivery to epithelial cells, we also found evidence for uptake of GFP by M cells (solid arrows in Fig. 3C–F) by all fusion tags. Again, these observations provide direct evidence for uptake of proteins in the upper gut after their lysis in the gut. Fig. 3E in particular illustrates the presence of GFP⁺ plant cells (“PC”) of CTB-GFP transplasmic plants near the site of delivery of released GFP to epithelial cells (“EC”) and M cells (solid arrow) of the ileum. For DCpep-GFP, no GFP⁺ epithelial cells were observed. However, we found examples of co-localization of GFP and M cells (Fig. 3F), suggesting that systemic delivery of DCpep-GFP is possible due to transport from the gut lumen via M cells. GFP delivered with all three tags showed accumulation in the liver (Fig. 3H, J and L), as expected because the blood can carry antigens from the gut to the liver via the portal vein (“gut-liver-axis”).

3.3. Purification of GFP fused with different tags

To study uptake of GFP by different cell types, the GFP fusion proteins were purified using toyopearlbutyl column for PTD-GFP and DCpep-GFP, and Ni²⁺ column for CTB-GFP. To examine the purity, densitometry was done using western blots and GFP standard (Fig. 4A). The purity of each tag fused GFP was ~95% for PTD-GFP, ~52% for DCpep-GFP, and ~13% for CTB-GFP. The variation in purity levels is attributed to the differences in the expression levels of each tag which is reflected on the recovered GFP fusion proteins after purification. Because proteins are purified based on hydrophobic interaction, other hydrophobic proteins could be present in the purified fractions. The purification of CTB-GFP was done with affinity Ni²⁺ column. Histidine cluster is generated when pentameric structure of CTB is formed, then the imidazole rings in the histidine cluster interact with Ni²⁺ [46]. The low purity of CTB-GFP is due to less stringent wash step, but increasing the stringency was accompanied with higher loss of the fused protein.

Purified GFP fusion proteins in SDS-PAGE and Coomassie stained gels showed distinct bands for each fusion protein at expected sizes, 29.2 kDa, 28.3 kDa and 39.5 kDa, for PTD-GFP, DCpep-GFP and CTB-GFP, respectively, (Fig. 4B). In case of PTD-GFP, there are two bands around at the expected size, which were 29.2 and 28.3 kDa. It has been reported that the C-terminal tail (His-Gly-Met-Asp-Glu-Tyr-Lys) of GFP is quite susceptible to proteolytic cleavage by carboxypeptidases and by nonspecific proteases including proteinase K and pronase, and various isoforms, caused by partial proteolytic cleavage, generated by ion exchange chromatography, isoelectric focusing, and native gel electrophoresis [47]. In order to determine GFP fluorescence, non-denaturing SDS-PAGE was performed where the fluorescence intensity was strongest in PTD-GFP (Lane 1) (Fig. 4C). In DCpep-GFP (Lane 2) 3 distinct proteins were seen with the top band most likely representing dimerized GFP [47] and the same was observed in PTD-GFP although it was of much higher intensity. The CTB-GFP fusion showed a set of larger fluorescence bands (Lane 3) starting from 190 kDa which corresponds to the pentamerization of CTB fused GFP and the other higher bands likely representing multimers. At the same lane, a smaller fragment slightly lower than the GFP standards was observed which could be a differently folded product similar to what was observed in PTD-GFP and DCpep-GFP.

To evaluate proper formation of pentameric structure of purified CTB-GFP, GM1 binding assay was performed with anti-CTB and anti-GFP antibody. It is well known that the pentameric structure of CTB has strong binding affinity to ganglioside GM1 receptors which are found ubiquitously on the surface of mammalian cells [48]. As seen in Fig. 4D, only CTB and CTB-GFP showed binding affinity, indicating complex formation between CTB and GM1. Also, the interaction of GM1-CTB-GFP was reconfirmed using anti-GFP antibody. Only CTB-GFP can be detected (Fig. 4E). To further confirm the pentameric structure of CTB-GFP, the purified CTB-GFP was run on the modified Tris-tricine gels under the non-denaturing conditions [36] and probed using anti-CTB antibody. The expected pentameric CTB-GFP form was detected at ~200 kDa along with the monomeric form at 39.5 kDa (Fig. 4F). It is likely that the monomer is dissociated from the oligomeric structure during the run due to SDS, which was added in the gel and electrophoresis buffer. Therefore, the CTB-GFP fusion protein formed the pentameric structure and retained ability

to bind to GM1 receptors, but there is no GM1 binding affinity for PTD-GFP or DCpep-GFP fusion protein.

3.4. Uptake of GFP fused with different tags by human immune and non-immune cells

Purified GFP fusion proteins were incubated with human cultured cells. Blood monocyte-derived mature DC, T cells (Jurkat cell), B cells (BCBL1), differentiated macrophages and mast cells were cultured for *in vitro* studies. Human kidney cells (HEK293T) and human pancreatic epithelioid carcinoma cells (PANC-1) were tested in parallel as examples of non-immune cells. Cells (2×10^4) were incubated with purified CTB, PTD and DC target peptide fused GFP for one hour at 37°C. Upon incubation with DCpep-GFP, intracellular GFP signal was detected only in DCs and not for any of the other cell type, confirming its specificity (Fig. 5A). PTD-GFP entered kidney cells or pancreatic cells but failed to enter any of the immune modulatory cells (Fig. 5A). PTD sequence was derived from PDX1 that induces insulin expression in pancreatic cells, and the exogenous PDX1 could penetrate mouse insulinoma cell line and activated insulin gene [41]. As expected, strong GFP signal was observed from PANC-1 cells when incubated with purified PTD-GFP. Also, PTD-GFP was observed in nucleus of the pancreatic ductal epithelial cells (Fig. 5B). The cell penetrating ability of PTD was also evident in human kidney cell line (Fig. 5A). In sharp contrast, GFP signals were detected in all cell types upon incubation with CTB-GFP, consistent with ubiquitous presence of GM1 receptors (Fig. 5A). Bone marrow-derived murine mast cells (a cell type that plays important roles in wound healing, defense to pathogens, and allergic reactions) showed no internalization of GFP delivered by DCpep or PTD, while CTB fused GFP was efficiently taken up (Fig. 5A). Although only one representative image is presented here, the uptake studies were performed in triplicates and 15–20 images for each cell line were recorded under confocal microscopy. CTB-GFP was observed in 70–92% of all the cell types examined and the variations are due to differences in cell density resulting in lower availability of GFP for their uptake. In case of PTD-GFP, no uptake (0%) was observed in any other cell type except kidney and pancreatic cells. DCpep-GFP was not observed in any other cell type (0%) except in dendritic cells (Table 1). This study offers specificity to deliver protein drugs to sera, immune system or specific organs or tissues, thereby facilitating further advancement of this novel concept.

4. Discussion

In our previous publications [6–16], we have shown that plant cell-derived proteins fused with CTB can be delivered across the intestinal epithelium for various applications, including delivery of functional proteins to the circulatory system and of protein antigens to the immune system (for oral tolerance induction or as a booster vaccine). This is possible because of binding of CTB pentamers to the GM1 receptors on the surface of gut epithelial and M cells, followed by transcytosis. However, GM1 is widely expressed by many different cell types and it is difficult to target to specific cell types. Therefore, in this study we sought to develop alternative tags that result in either more cell type-specific and/or more efficient transmucosal delivery. We chose DCpep as an example for specific delivery to professional antigen presenting cells and were able to confirm its specificity. PTD not only delivers the GFP cargo more effectively to the circulation via penetration of intestinal

epithelial cells (Fig. 3A and C) but totally avoids delivery to immune cells (Fig. 5A). In our opinion, data presented here on PTD are paradigm shift in drug delivery, in sharp contrast to previous assumptions that they are non-specific.

Given recent disagreements in the literature about mechanisms of cell penetration by PTDs (macropinocytosis vs direct transfer) and about effects of PTDs vs the cargo they carry [49], this is a very timely contribution to this field. Our data show that the body's immune system can be excluded from protein drug delivery by specific choice of PTD, while efficiently delivering to other cell types and circulation. Thus, this study is likely to spark new investigations on screening of PTDs and determining their specificity. Combined with sequence and structural knowledge, this will hopefully lead to custom-designed PTDs in the future. We used defined in vitro systems to demonstrate the differences in protein transduction between different tags as a function of the target cell type. Future studies will focus on immunological consequences, using disease-specific antigens instead of GFP and corresponding animal models.

To reveal routes by which the GFP fusion proteins cross the intestinal epithelial layer and delivery to circulation and biodistribution to other organs, the immunostaining studies of small intestine tissue sections after oral delivery of leaf materials expressing three GFP tag proteins were carried out. CTB was confirmed to be targeted to GM1 receptors on epithelial cells and by M cells. Our study found that PTD is able to penetrate non-immune cells, which explains why this tag also transfers GFP to epithelial cells. In contrast, DC peptide is a specific ligand to dendritic cells and therefore should not target epithelial cells. However, our data show that uptake by M cells is a mechanism of entry for DCpep fusions, thus explaining how systemic delivery of DCpep-GFP is possible via the oral route. Dendritic cells are also directly targeted by DCpep through their protrusions between epithelial cells. However, the amounts of gut luminal antigen sampled by this mechanism are too small to be visualized.

We expect that protein antigens released from CTB after transcytosis are taken up by DC (and to a lesser extent by macrophages) in the gut immune system (as we have extensively published) and that DCpep-GFP translocated by M cells is also taken up by DC. However, for initial studies of interactions with immune cells, we utilized a more sensitive and defined in vitro approach using cultured human cells. Future investigations will address antigen uptake and processing in vivo and the resulting immune responses.

4.1. Is CTB fusion ideal for oral immune modulatory therapy?

CTB fusion delivered GFP to all tested tissues and cell types including non-immune and immune cells. It is well established that CTB specifically binds with GM1 ganglioside and lots of CTB-fused proteins expressed in chloroplasts in our lab also showed the strong binding affinity to GM1 [6, 8, 9, 13–16]. CTB travels retrograde through the trans-Golgi Network into the endoplasmic reticulum (ER) for cell entry once CTB binds with GM1, enriched in membrane lipid rafts of intestinal epithelial cells [50, 51]. In fact, CTB has been widely used as a probe to quantitatively study GM1 and its cellular and subcellular distribution [52]. The use of CTB as a transmucosal carrier can facilitate the transportation of conjugated proteins into circulation through its strong binding affinity to GM1 and the

large mucosal area of human intestine (approximately 1.8–2.7 m² against body weight [53]. Up to 15,000 CTB molecules can bind to one intestinal epithelial cell at a time [54] and the GM1 receptor turns over rapidly on the cell surface [55]. Furthermore, GM1 gangliosides are also found in the plasma membranes of many other cell types, with particular abundance in the nervous system and retina [56, 57], thus directing efficient uptake of CTB fusion protein in these cells.

Our strategy of oral tolerance induction to autoantigens and to therapeutic proteins used in replacement therapy of genetic disorder (such as hemophilia and lysosomal storage disorders) has in part relied on efficient targeting of gut epithelial cells with CTB followed by transmucosal delivery and proteolytic cleavage, resulting in the release of the antigen from the CTB tag and uptake by DCs [7, 9, 10, 11, 33,]. However, DCs and macrophages also directly sample antigen in the gut lumen, and M cells may shuttle intact antigen across the epithelium to areas rich in DCs. Our new data show that CTB fusions are efficiently taken up by DC, macrophages, and other immune cells, providing an additional explanation for the effectiveness of CTB fused antigens in plant-based immune modulatory protocols.

We had also used CTB fusions effectively as oral booster vaccines against pathogens after initial priming in the presence of aluminum adjuvant [46]. However, when primed with adjuvant, CTB is highly immunogenic and therefore diverts the specific response from antigen of interest [46, 58], limiting its use in vaccine development. Aggregation of protein antigens due to formation of multimers or pentamers and size restrictions of this transmucosal carrier are additional potential limitations. Determination of antigen dose is yet another major challenge because this would require complete solubilization of CTB pentamers. Therefore, there is a need to explore other pathways for oral delivery and investigate the point of entry of protein antigens. Accurate targeting of therapeutic proteins to a specific tissue minimizes side effects and increases efficacy, which eventually increases therapeutic benefit to patients.

4.2. Specific targeting of dendritic cells by DCpep ideal for delivery to the immune system

Here, we introduce an alternative and more specific peptide sequence with high potential for immunotherapy. DCpep specifically targets DCs but not any other immune cells or non-immune cells. To assess translational implications, we mostly used human immune cells to differentiate targeting characteristics of the fusion tags. DCpep only delivered intact GFP antigen to DCs but not any other APCs or immune cells or non-immune cells. Consistent with this finding, DCpep-GFP failed to target gut epithelial cells *in vivo*. Systemic delivery most likely resulted from uptake by M cells. Going forward, one can now design immune tolerance and vaccine protocols based on specific delivery to DC, which have critical functions in Treg induction and immune stimulation, depending on activation signals.

As we know, the delivery of antigens to lymph node is quite important for immunotherapy. However, this aspect cannot be directly demonstrated by GFP signal because proteins taken up by DC in the lamina propria or Peyer's patches are fragmented into small peptides and loaded onto MHC molecules by the time the DC have migrated to the lymph nodes for presentation of antigen to T cells. In agreement with the notion that mesenteric lymph nodes (MLN) are critical in their response to ingested antigens, we recently demonstrated increases

in different DC subsets and induction of Treg in the MLNs of mice that received oral delivery of transplastic plant cells [10].

4.3. PTD is ideal for efficient systemic delivery via the oral route excluding the immune system

While CTB fusions effectively target the gut immune system and are thus useful for tolerance induction, an alternative strategy to avoid immune complications is to minimize interactions with the immune system. The protein transduction domain of PDX-1 exhibited unique selectivity in the transfer of GFP to different cell types. PTD-GFP entirely failed to deliver antigen to APCs and lymphocytes but was able to transfer GFP to non-immune cells (including gut epithelial cells *in vivo*). Since myeloid and lymphoid cells are hematopoietic cells, it is possible that PDX-1 fails to transduce this specific cell lineage. PDX-1 induces insulin expression upon protein transduction via macropinocytosis, a specialized form of endocytosis that is distinct from receptor-mediated uptake [59, 60]. Macropinocytosis is also major mechanism of uptaking macromolecules in kidney, so the observation of GFP signals in HEK293T after incubation with purified PTD-GFP could be the consequence of the endocytosis induced by PTD. Lack of GFP signal in immune cells after incubation with PTD-GFP cannot be explained by enhanced degradation after uptake but rather reflects a failure of protein transduction of these cells because i) there was also a lack of binding to the cell surface, and ii) the PTD of HIV tat, which also utilizes the macropinocytosis mechanism, readily delivers intact GFP into human DC and other APCs by the PTD of HIV tat [61–63]. PTD derived from PDX-1 clearly displays a distinct selectivity for cellular transduction, possibly related to surface properties of the target cell membrane. Although both PTDs enter the cell by macropinocytosis, their amino acid sequences are very different, which is likely to affect cell surface binding. While infection of lymphocytes is a critical step of the HIV life cycle, insulin expression needs to be tightly regulated and responsive to environmental stimuli [64], which may in part account for the selectivity of PTD from PDX-1. At the same time, PTD-GFP was superior *in vivo* for systemic protein delivery, which can be exploited for therapies that require certain protein levels in the blood, such as in our published examples of treatment of hypertension and hormone or cytokine therapies [9, 11, 14, 15]. Interestingly, despite marked differences in systemic delivery, CTB-, DCpep-, and PTD-tags all resulted in very similar GFP antigen levels in the liver, as evidenced by immunohistochemistry and more quantitatively by ELISA. Links between responses in the gut and the liver have long been known and are often referred to as the “gut-liver axis”. Upon uptake by the gut, antigen can traffic to the liver indirectly via migratory DC that is routed through the mesenteric lymph node. Alternatively, the blood can carry antigens from the gut to the liver via the portal vein. Given the broad distribution of quantifiable levels of GFP in the liver, the latter explanation seems more likely for our delivery system. The data suggest that the liver takes up the orally delivered antigen to a level of saturation that is less dependent on the tag.

4.4. Unique advantages of delivery of proteins bioencapsulated in plant cells

Lyophilization of plant cells has several advantages. The freeze-dried powdered leaves can be stored at room temperature for years eliminating expensive cold storage and transportation which are required for injectable protein drugs [13, 65]. Also, concentration

effect of the therapeutic protein is increased facilitating 10–20 fold reduction in the size of capsules containing lyophilized plant cells. Freeze drying technology is widely used to preserve protein drugs by the pharmaceutical industry, including preservation of blood clotting factors. So, freeze drying process doesn't denature proteins. Indeed, we have repeatedly shown that freeze drying preserves proper folding and disulfide bonds (11, 13–16, 66). Upon oral delivery, lyophilized plant cells reach the intestine, and the bioencapsulated proteins are released by gut microbes through digestion of plant cell wall. That time, the released proteins as well as plant cell walls can be degraded by gut microbes. However, it is possible that the gut microbiome is enriched by anaerobic bacteria that release more enzymes to degrade plant cell wall than protein degradation. Bacteria inhabiting the human gut have indeed evolved to utilize complex carbohydrates in plant cell wall and are capable of utilizing almost all plant glycans [4, 5]. Our previously published work identified enzymes that are required to breakdown plant cell wall [67, 68]. Delivery of several functional proteins show that they are either protected in the gut lumen or adequate quantities of protein drugs are released that survive gut lumen proteases.

DCpep-GFP content was found to be the lowest among three fusion proteins, 2.16 µg/mg, which is 10 times lower than that of PTD-GFP. Generally, chloroplast expression of foreign protein can reach very high level, up to 70% of total leaf proteins [7] due to high copy number of chloroplast genome. However, expression level varies based on protein, N-terminal fusions, proteolytic cleavage and stability. In this study, all the chimeric genes were driven by the *psbA* promoter and *psbA* 5 UTR, and stabilized *psbA* 3 UTR. Since the GFP sequence is also same among all three constructs, the contributing factors that affect the difference of the expression level could be due to the N-terminal sequence of the fusion constructs. In contrast to PTD and CTB tag, DCpep was fused to C-terminal of GFP. Therefore, one possible explanation for lower level of GFP expression of DCpep fusion is inadequate protection of the N-terminus.

5. Conclusions

As illustrated above, bioavailability of oral delivery of protein drugs expressed in genetically modified plant cells is now emerging as a new concept for inducing tolerance against autoimmune disorders [7] or to eliminate toxicity of injected protein drugs [8–10] or deliver functional blood proteins to treat diabetes [12, 13], hypertension [14], protection against retinopathy [15] or removal of plaques in Alzheimer's brain [16]. These novel approaches should improve patient compliance in addition to significantly lowering the cost of healthcare as seen in the diabetes study in which oral delivery was as effective as injectable delivery to lower blood glucose levels using insulin or exendin-4 [12, 13].

This study has enabled utilization of different fusion tags to deliver either to immune modulatory cells or non-immune cells or directly to sera without interfering with the immune system. This opens up the potential for low cost oral delivery of proteins to enhance or suppress immunity or functional proteins to regulate metabolic pathways.

The cost of protein drugs now exceeds GDP of >75% of countries, making them unaffordable. This is because of their production in prohibitively expensive fermenters,

purification, cold storage/transportation, short shelf life and sterile delivery methods. Using green fluorescent protein (GFP) as a model, we demonstrate in this study that plant cells protect GFP from the digestive system and release it into the gut lumen where they are absorbed by epithelial cells. Based on the delivery tag fused to GFP, they reach the circulatory system, immune cells or non-immune cells, specific organs or tissues. Such low cost oral delivery of protein drugs should increase patient compliance and dramatically lower their cost by elimination of currently used prohibitively expensive processes/injections.

Acknowledgments

Research presented here is supported in part by NIH grants R01 GM 63879, R01 HL 109442, and R01 HL 107904 to Henry Daniell. We thank Dr. Weissman Drew, Dr. Anil Rustgi (Perelman school of medicine, university of Pennsylvania), Dr. Yuan Yan, Dr. Kathleen Battaglia, Dr. Hydar Ali (School of Dental Medicine, university of Pennsylvania), Dr. Janis Burkhardt (Children's Hospital of Philadelphia Research Institute) for providing us Dendritic, pancreatic, B (BCBL1), macrophage, mast, and T cells. Authors thank Akhil Kotian and Aalok Shah from the Daniell lab for providing mast cell data in Fig. 5 and assistance with pancreatic cell line experiments.

References

- Walsh G. Biopharmaceutical benchmarks 2014. *Nature Biotechnology*. 2014; 32:992–1000.
- Jin S, Daniell H. Engineered chloroplast genome just got smarter. *Trends in Plant Science*. 2015; 20:622–640. [PubMed: 26440432]
- Chan HT, Daniell H. Plant-made vaccines against human infectious diseases-Are we there yet? *Plant Biotechnol J*. 2015; 13:1056–1070. [PubMed: 26387509]
- Martens EC, Lowe EC, Chiang H, Pudlo NA, Wu M, McNulty NP, et al. Recognition and degradation of plant cell wall polysaccharides by two human gut symbionts. *PLoS Biol*. 2011; 9:e1001221. [PubMed: 22205877]
- Flint HJ, Bayer EA, Rincon MT, Lamed R, White BA. Polysaccharide utilization by gut bacteria: potential for new insights from genomic analysis. *Nat Rev Microbiol*. 2008; 6:121–131. [PubMed: 18180751]
- Limaye A, Koya V, Samsam M, Daniell H. Receptor-mediated oral delivery of a bioencapsulated green fluorescent protein expressed in transgenic chloroplasts into the mouse circulatory system. *FASEB J*. 2006; 20:959–961. [PubMed: 16603603]
- Ruhlman T, Ahangari R, Devine A, Samsam M, Daniell H. Expression of cholera toxin B-proinsulin fusion protein in lettuce and tobacco chloroplasts--oral administration protects against development of insulinitis in non-obese diabetic mice. *Plant Biotechnol J*. 2007; 5:495–510. [PubMed: 17490448]
- Verma D, Moghimi B, LoDuca PA, Singh HD, Hoffman BE, Herzog RW, et al. (2010) Oral delivery of bioencapsulated coagulation factor IX prevents inhibitor formation and fatal anaphylaxis in hemophilia B mice. *Proc Natl Acad Sci USA*. 2010; 107:7101–7106. [PubMed: 20351275]
- Sherman A, Su J, Lin S, Wang X, Herzog RW, Daniell H. Suppression of inhibitor formation against FVIII in a murine model of hemophilia A by oral delivery of antigens bioencapsulated in plant cells. *Blood*. 2014; 124:1659–1668. [PubMed: 24825864]
- Wang X, Su J, Sherman A, Rogers GL, Liao G, Hoffman BE, et al. Plant-based oral tolerance for hemophilia results from a complex immune regulatory mechanism including LAP⁺CD4⁺ T cells. *Blood*. 2015; 125:2418–2427. [PubMed: 25700434]
- Su J, Sherman A, Doerfler PA, Byrne BJ, Herzog RW, Daniell H. Oral delivery of Acid Alpha Glucosidase epitopes expressed in plant chloroplasts suppresses antibody formation in treatment of Pompe mice. *Plant Biotechnol J*. 2015; 13:1023–1032. [PubMed: 26053072]
- Boyhan D, Daniell H. Low-cost production of proinsulin in tobacco and lettuce chloroplasts for injectable or oral delivery of functional insulin and C-peptide. *Plant Biotechnol J* 2011. 2011; 9:585–598.

13. Kwon KC, Nityanandam R, New JS, Daniell H. Oral delivery of bioencapsulated exendin-4 expressed in chloroplasts lowers blood glucose level in mice and stimulates insulin secretion in beta-TC6 cells. *Plant Biotechnol J*. 2013; 11:77–86. [PubMed: 23078126]
14. Shenoy V, Kwon KC, Rathinasabapathy A, Lin S1, Jin G, Song C, et al. Oral delivery of Angiotensin-converting enzyme 2 and Angiotensin-(1-7) bioencapsulated in plant cells attenuates pulmonary hypertension. *Hypertension*. 2014; 64:1248–1259. [PubMed: 25225206]
15. Shil PK, Kwon KC, Zhu P, Verma A, Daniell H, Li Q. Oral Delivery of ACE2/Ang-(1-7) Bioencapsulated in Plant Cells Protects against Experimental Uveitis and Autoimmune Uveoretinitis. *Molecular Therapy*. 2014; 22:2069–2082. [PubMed: 25228068]
16. Kohli N, Westerveld DR, Ayache AC, Verma A, Shil P, Prasad T, et al. Oral Delivery of Bioencapsulated Proteins Across Blood-Brain and Blood-Retinal Barriers. *Molecular Therapy*. 2014; 22:535–546. [PubMed: 24281246]
17. Zahid M, Robbins PD. Protein transduction domains: applications for molecular medicine. *Curr Gene Ther*. 2012; 12:374–380. [PubMed: 22920684]
18. Khaja K, Robbins P. Comparison of Functional Protein Transduction Domains Using the NEMO Binding Domain Peptide. *Pharmaceuticals*. 2010; 3:110–124.
19. Embury J, Klein D, Pileggi A, Ribeiro M, Jayaraman S, Molano RD, et al. Proteins linked to a protein transduction domain efficiently transduce pancreatic islets. *Diabetes*. 2001; 50:1706–1713. [PubMed: 11473028]
20. Schwarze SR, Ho A, Vocero-Akbani A, Dowdy SF. In vivo protein transduction: delivery of a biologically active protein into the mouse. *Science*. 1999; 285:1569–1572. [PubMed: 10477521]
21. Mills CD. M1 and M2 Macrophages: Oracles of Health and Disease. *Critical Reviews in immunology*. 2012; 32:463–488. [PubMed: 23428224]
22. Banchereau J, Steinman RM. Dendritic cells and the control of immunity. *Nature*. 1998; 392:245–252. [PubMed: 9521319]
23. Ingulli E, Mondino A, Khoruts A, Jenkins MK. In vivo detection of dendritic cell antigen presentation to CD4+ T cells. *J Exp Med*. 1997; 185:2133–2141. [PubMed: 9182685]
24. Luther SA, Gulbranson-Judge A, Acha-Orbea H, MacLennan ICM. Viral superantigen drives extrafollicular and follicular B differentiation leading to virus-specific antibody production. *J Exp Med*. 1997; 185:551–562. [PubMed: 9053455]
25. Kudo S, Matsuno K, Ezaki T, Ogawa M. A novel migration pathway for rat dendritic cells from the blood: Hepatic sinusoids-lymph translocation. *J Exp Med*. 1997; 185:777–784. [PubMed: 9034155]
26. Curiel TJ, Morris C, Brumlik M, Landry SJ, Finstad K, Nelson A, et al. Peptides identified through phage display direct immunogenic antigen to dendritic cells. *J Immunol*. 2004; 172:7425–7431. [PubMed: 15187120]
27. Banchereau J, Palucka AK. Dendritic cells as therapeutic vaccines against cancer. *Nat Rev Immunol*. 2005; 5:296–306. [PubMed: 15803149]
28. Celluzzi CM, Mayordomo JI, Storkus WJ, Lotze MT, Falo LD Jr. Peptide-pulsed dendritic cells induce antigen-specific CTL-mediated protective tumor immunity. *J Exp Med*. 1996; 183:283–287. [PubMed: 8551233]
29. Kraehenbuhl JP, Corbett M. Immunology. Keeping the gut microflora at bay. *Science*. 2004; 303:1624–1625. [PubMed: 15016988]
30. von Boehmer H. Oral tolerance: is it all retinoic acid? *J Exp Med*. 2007; 204:1737–1739. [PubMed: 17620364]
31. Weiner HL. Oral tolerance: immune mechanisms and treatment of autoimmune diseases. *Immunol Today*. 1997; 18:335–343. [PubMed: 9238837]
32. Annacker O, Coombes JL, Malmstrom V, Uhlig HH, Bourne T, Johansson-Lindbom B, et al. Essential role for CD103 in the T cell-mediated regulation of experimental colitis. *J Exp Med*. 2005; 202:1051–1061. [PubMed: 16216886]
33. Biswas M, Sarkar D, Kumar SR, Nayak S, Rogers GL, Markusic DM, et al. Synergy between rapamycin and FLT3 ligand enhances plasmacytoid dendritic cell-dependent induction of CD4+CD25+FoxP3+ Treg. *Blood*. 2015; 125:2937–2947. [PubMed: 25833958]

34. Kwon KC, Verma D, Jin S, Singh ND, Daniell H. Release of proteins from intact chloroplasts induced by reactive oxygen species during biotic and abiotic stress. *PLoS One*. 2013c; 8:e67106. [PubMed: 23799142]
35. Verma D, Samson NP, Koya V, Daniell H. A protocol for expression of foreign genes in chloroplasts. *Nat Protoc*. 2008; 3:739–758. [PubMed: 18388956]
36. Haider SR, Sharp BL, Reid HJ. A comparison of Tris-glycine and Tris-tricine buffers for the electrophoretic separation of major serum proteins. *J Sep Sci*. 2011; 34:2463–2467. [PubMed: 21818850]
37. Lee S, Li B, Jin S, Daniell H. Expression and characterization of antimicrobial peptides Retrocyclin-101 and Protegrin-1 in chloroplasts to control viral and bacterial infections. *Plant Biotechnol J*. 2011; 9:100–115. [PubMed: 20553419]
38. Sanchez J, Holmgren J. Cholera toxin - a foe & a friend. *Indian J Med Res*. 2011; 133:153–163. [PubMed: 21415489]
39. Magzoub M, Eriksson LE, Gräslund A. Conformational states of the cell-penetrating peptide penetratin when interacting with phospholipid vesicles: effects of surface charge and peptide concentration. *Biochim Biophys Acta*. 2002; 1563:53–63. [PubMed: 12007625]
40. Roy A, Kucukural A, Zhang Y. I-TASSER: a unified platform for automated protein structure and function prediction. *Nature Protocols*. 2010; 5:725–738. [PubMed: 20360767]
41. Noguchi H, Kaneto H, Weir GC, Bonner-Weir S. PDX-1 protein containing its own antennapedia-like protein transduction domain can transduce pancreatic duct and islet cells. *Diabetes*. 2003; 52:1732–1737. [PubMed: 12829640]
42. Hessabi B, Ziegler P, Schmidt I, Hessabi C, Walther R. The nuclear localization signal (NLS) of PDX-1 is part of the homeodomain and represents a novel type of NLS. *Eur J Biochem*. 1999; 263:170–177. [PubMed: 10429201]
43. Phillips GN Jr. Structure and dynamics of green fluorescent protein. *Curr Opin Struct Biol*. 1997; 7:821–827. [PubMed: 9434902]
44. Miyata T, Oshiro S, Harakuni T, Taira T, Matsuzaki G, Arakawa T, et al. Physicochemically stable cholera toxin B subunit pentamer created by peripheral molecular constraints imposed by de novo-introduced intersubunit disulfide crosslinks. *Vaccine*. 2012; 30:4225–4232. [PubMed: 22542816]
45. Lakshmi PS, Verma D, Yang X, Lloyd B, Daniell H. Low cost tuberculosis vaccine antigens in capsules: expression in chloroplasts, bio-encapsulation, stability and functional evaluation in vitro. *PLoS One*. 2013; 8:e54708. [PubMed: 23355891]
46. Davoodi-Semiromi A, Schreiber M, Nalapalli S, Verma D, Singh ND, Banks RK, et al. Chloroplast-derived vaccine antigens confer dual immunity against cholera and malaria by oral or injectable delivery. *Plant Biotechnol J*. 2010; 8:223–242. [PubMed: 20051036]
47. William, WW. Biochemical and physical properties of green fluorescent protein. In: Chalfie, M.; Kain, SR., editors. *Green fluorescent protein*. 2. Hoboken; New Jersey: 2006. p. 39-65.
48. Daniell H, Lee SB, Panchal T, Wiebe PO. Expression of the native cholera toxin B subunit gene and assembly as functional oligomers in transgenic tobacco chloroplasts. *J Mol Biol*. 2001; 311:1001–1009. [PubMed: 11531335]
49. Durzy ska J, Przysiecka Ł, Nawrot R, Barylski J, Nowicki G, Warowicka A, Musidlak O, Go dzicka-Józefiak A. Viral and other cell-penetrating peptides as vectors of therapeutic agents in medicine. *J Pharmacol Exp Ther*. 2015; 354:32–42. [PubMed: 25922342]
50. Wernick NL, Chinnapen DJ, Cho JA, Lencer WI. Cholera toxin: an intracellular journey into the cytosol by way of the endoplasmic reticulum. *Toxins (Basel)*. 2010; 2:310–325. [PubMed: 22069586]
51. Cho JA, Chinnapen DJ, Amar E, te Welscher YM, Lencer WI, Massol R. Insights on the trafficking and retro-translocation of glycosphingolipid-binding bacterial toxins. *Front Cell Infect Microbiol*. 2012; 2:51. [PubMed: 22919642]
52. Critchley DR, Kellie S, Streuli CH, Patel B, Ansell S, Pierce E, et al. The use of cholera toxin as a probe to study the organisation of ganglioside GM1 in membranes. *Prog Clin Biol Res*. 1982; 102(pt A):397–407. [PubMed: 7167449]
53. Wilson JP. Surface area of the small intestine in man. *Gut*. 1967; 8:618–621. [PubMed: 5625041]

54. Holmgren J, Lönnroth I, Månsson J, Svennerholm L. Interaction of cholera toxin and membrane GM1 ganglioside of small intestine. *Proc Natl Acad Sci USA*. 1975; 72:2520–2524. [PubMed: 1058471]
55. Fishman PH, Bradley RM, Hom BE, Moss J. Uptake and metabolism of exogenous gangliosides by cultured cells: effect of cholera toxin on the turnover of GM1. *J Lipid Res*. 1983; 24:1002–1011. [PubMed: 6631229]
56. Hadjiconstantinou M, Neff NH. GM1 ganglioside: in vivo and in vitro trophic actions on central neurotransmitter systems. *J Neurochem*. 1998; 70:1335–1345. [PubMed: 9523549]
57. Yu RK, Tsai YT, Ariga T. Functional roles of gangliosides in neurodevelopment: an overview of recent advances. *Neurochem Res*. 2012; 37:1230–1244. [PubMed: 22410735]
58. Yu J, Langridge WH. A plant-based multicomponent vaccine protects mice from enteric diseases. *Nat Biotechnol*. 2001; 19:548–552. [PubMed: 11385459]
59. Noguchi H, Matsushita M, Matsumoto S, Lu YF, Matsui H, Bonner-Weir S, et al. Mechanism of PDX-1 protein transduction. *Biochem Biophys Res Commun*. 2005; 332:68–74. [PubMed: 15896300]
60. Noguchi H, Matsumoto S, Okitsu T, Iwanaga Y, Yonekawa Y, Nagata H, et al. PDX-1 protein is internalized by lipid raft-dependent macropinocytosis. *Cell Transplant*. 2005; 14:637–645. [PubMed: 16405074]
61. Kaplan IM, Wadia JS, Dowdy SF. Cationic TAT peptide transduction domain enters cells by macropinocytosis. *J Control Release*. 2005; 102:247–253. [PubMed: 15653149]
62. Batchu RB, Moreno AM, Szmania SM, Bennett G, Spagnoli GC, Ponnazhagan S, et al. Protein transduction of dendritic cells for NY-ESO-1-based immunotherapy of myeloma. *Cancer Res*. 2005; 65:10041–10049. [PubMed: 16267030]
63. Su Y, Zhang AH, Li X, Owusu-Boaitey N, Skupsky J, Scott DW. B cells “transduced” with TAT-fusion proteins can induce tolerance and protect mice from diabetes and EAE. *Clin Immunol*. 2011; 140:260–267. [PubMed: 21546313]
64. Calder PC, Dimitriadis G, Newsholme P. Glucose metabolism in lymphoid and inflammatory cells and tissues. *Curr Opin Clin Nutr Metab Care*. 2007; 10:531–540. [PubMed: 17563475]
65. Kwon KC, Verma D, Singh ND, Herzog R, Daniell H. Oral delivery of human biopharmaceuticals, autoantigens and vaccine antigens bioencapsulated in plant cells. *Adv Drug Deliv Rev*. 2013; 65:782–799. [PubMed: 23099275]
66. Su J, Zhu L, Sherman A, Wang X, Lin S, Kamesh A, Norikane JH, Streatfield SJ, Herzog RW, Daniell H. Low cost industrial production of coagulation factor IX bioencapsulated in lettuce cells for oral tolerance induction in hemophilia B. *Biomaterials*. 2015; 70:84–93. [PubMed: 26302233]
67. Agrawal P, Verma D, Daniell H. Expression of *Trichoderma reesei* β -mannanase in tobacco chloroplasts and its utilization in lignocellulosic woody biomass hydrolysis. *PLoS One*. 2011; 6:e29302. [PubMed: 22216240]
68. Verma D, Jin S, Kanagaraj A, Singh ND, Daniel J, Kolattukudy PE, Miller M, Daniell H. Expression of fungal cutinase and swollenin in tobacco chloroplasts reveals novel enzyme functions and/or substrates. *PLoS One*. 2013; 8:e57187. [PubMed: 23451186]

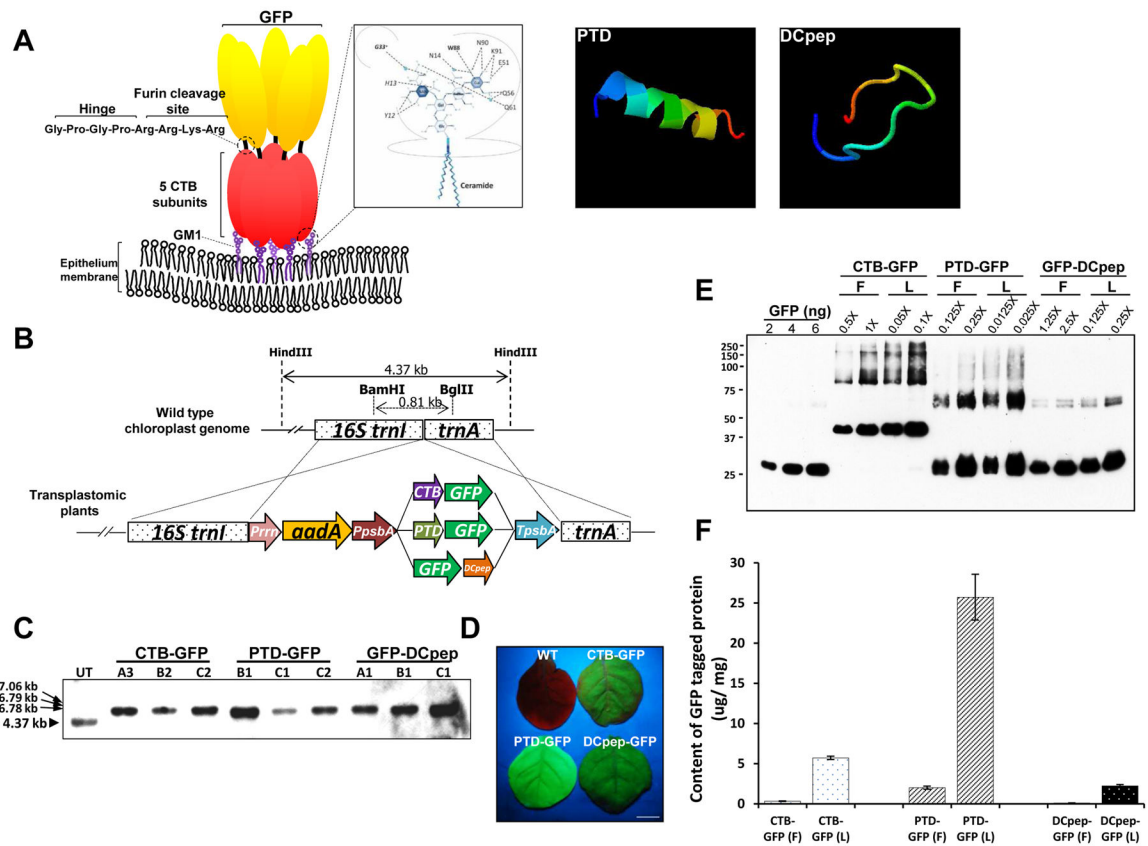


Fig. 1. Schematic diagrams for predicted protein structures and characterization of transplastomic lines expressing GFP-fusion proteins

(A) Interaction of CTB fusion protein and GM1 receptor, and predicted 3D structure of both PTD and DCpep. Pentasaccharide moiety of GM1 receptor establishes interaction with pentameric structure of CTB. The inset box shows atoms involved in the interaction between CTB and sugars in more detail [38]. The Hinge sequence for avoiding steric hindrance and furin cleavage site for releasing the tethered protein were placed between CTB and the fused protein. Computational predicted three-dimensional structures of both PTD and DCpep were obtained from iterative threading assembly refinement (I-TASSER) server [40]. The structure is shown in rainbow, where the color changes from blue to red gradually for residues from N-terminal to C-terminal (blue-green-yellow-orange-red). Among predicted structures, the model with the highest reliable structure for each peptide, which was chosen based on the combined results from parameter calculations such as confidence score (C-score), high-resolution models with root mean square deviation (RMSD) value, and template modeling score (TM-score), was presented. (B) Schematic diagram for expression cassette of GFP-fused carrier proteins and flanking regions. *Prrn*, rRNA operon promoter; *aadA*, aminoglycoside 3'-adenylyltransferase gene; *PpsbA*, promoter and 5' UTR of *psbA* gene; *CTB*, coding sequence of non-toxic cholera B subunit; *PTD*, coding sequence of protein transduction domain; *DCpep*, dendritic cell binding peptide sequence; *smGFP*, gene sequence for soluble-modified green fluorescent protein; *TpsbA*, 3' UTR of *psbA* gene; *trnI*, isoleucyl-tRNA; *trnA*, alanyl-tRNA. Restriction enzymes used for Southern blot analysis were indicated as *Bam*HI/*Bg*II for the generation of probe and *Hind*III for the digestion of

genomic DNA. **(C)** Southern blot analysis of each transplastomic line expressing GFP-fused tag proteins. *HindIII*-digested gDNAs were probed with the flanking region fragment described above. **(D)** GFP fluorescence signals from each transplastomic line were confirmed under UV light. The picture was taken after 2 months of germination. Bar represents 0.5 cm. **(E)** Western blot analysis for densitometric quantification with GFP standard proteins. Lyophilized (10 mg) and fresh leaf material (100 mg) were extracted in 300 μ L extraction buffer. 1X represents 1 μ L of homogenate resuspended in the extraction buffer in a ratio of 100 mg to 300 μ L. **(F)** Amount of GFP fusion proteins in fresh (F) and lyophilized (L) leaves. Data are means \pm SD of three independent experiments.

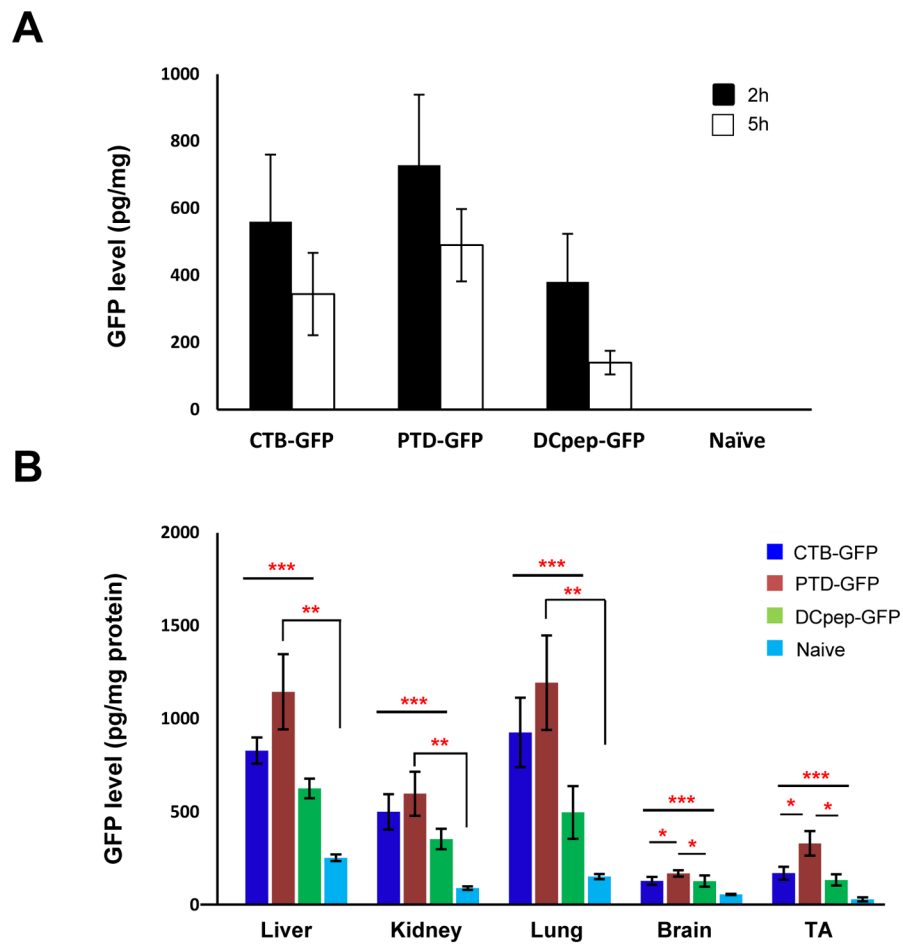


Fig. 2. Efficiency of oral delivery and biodistribution of GFP fused with different tags
 Serum (A) and tissue (B) GFP levels in mice (N=6 per group) fed leaf materials expressing CTB-GFP, PTD-GFP and DCpep-GFP. Adult mice were orally fed with leaf materials from transgenic tobacco plants, with the amount adjusted to GFP expression levels, for three consecutive days. A control group (N=6) kept unfed. Blood samples were collected at 2 and 5 hours after last gavage at which, mice were sacrificed and tissue samples were collected for protein isolation. GFP concentration in serum and tissues were measured with ELISA. The data was shown as average \pm SEM. Statistic significance was determined by a paired Student's *t* test, and *p* value less than 0.05 were considered significant. * $P < 0.05$, ** $P < 0.01$, *** $P < 0.05$ or $P < 0.01$ (CTD, PTD and DCpep versus Naïve)

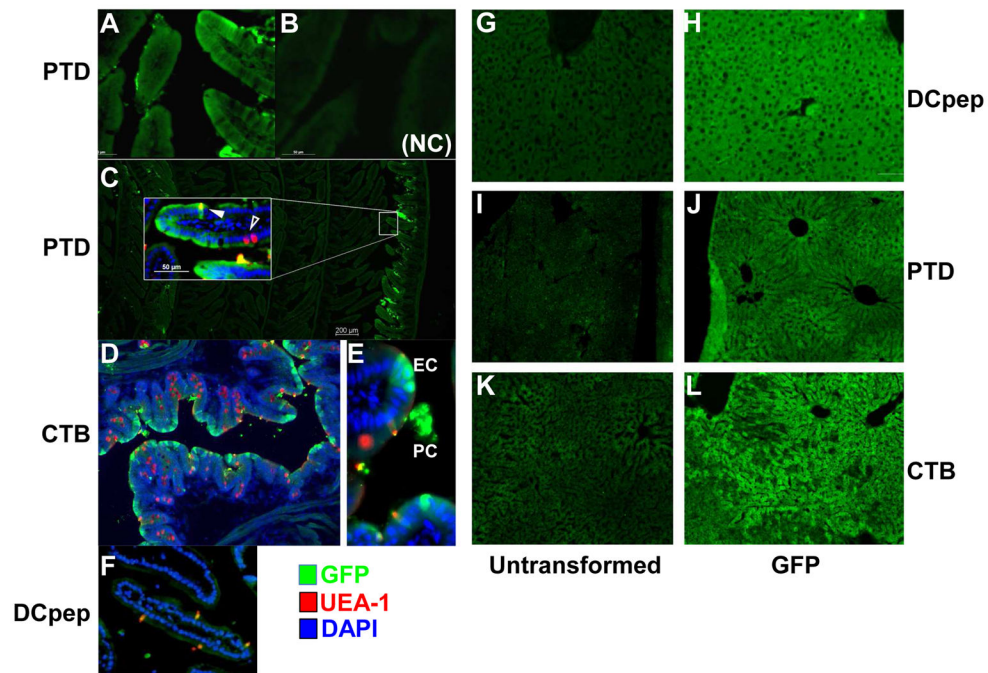


Fig. 3. Visualization of GFP in cells of ileum and liver of mice after oral delivery of plant cells
 GFP delivery to small intestine (left panel). Shown are cross-sections stained with anti-GFP (green signal; Alexa Fluor 488), UEA-1 (which stains, among other cells, M cells, red signal, rhodamine), and DAPI (nuclear stain, blue). (A–C). PTD-GFP delivery. (B) No primary antibody (NC: negative control). (D–E) CTB-GFP delivery. (F) DCpep delivery. Original magnification: 200x (A, B, D–F, insert in C) or 40x (C). GFP stain shown in liver's cryosection (right panel), identical exposure time during image capture. The primary antibody: rabbit anti-GFP antibody at 1:1000 and second antibody: Alexa Fluor 488 Donkey Anti-Rabbit IgG was used for GFP staining. (G, I and K) liver sections of mice fed with untransformed lyophilized plant cells. (H, J and L) GFP signals of liver sections from mice fed with lyophilized plant cells expressing DCpep-GFP (H), PTD-GFP (J), and CTB-GFP (L). Original magnification: 100x.

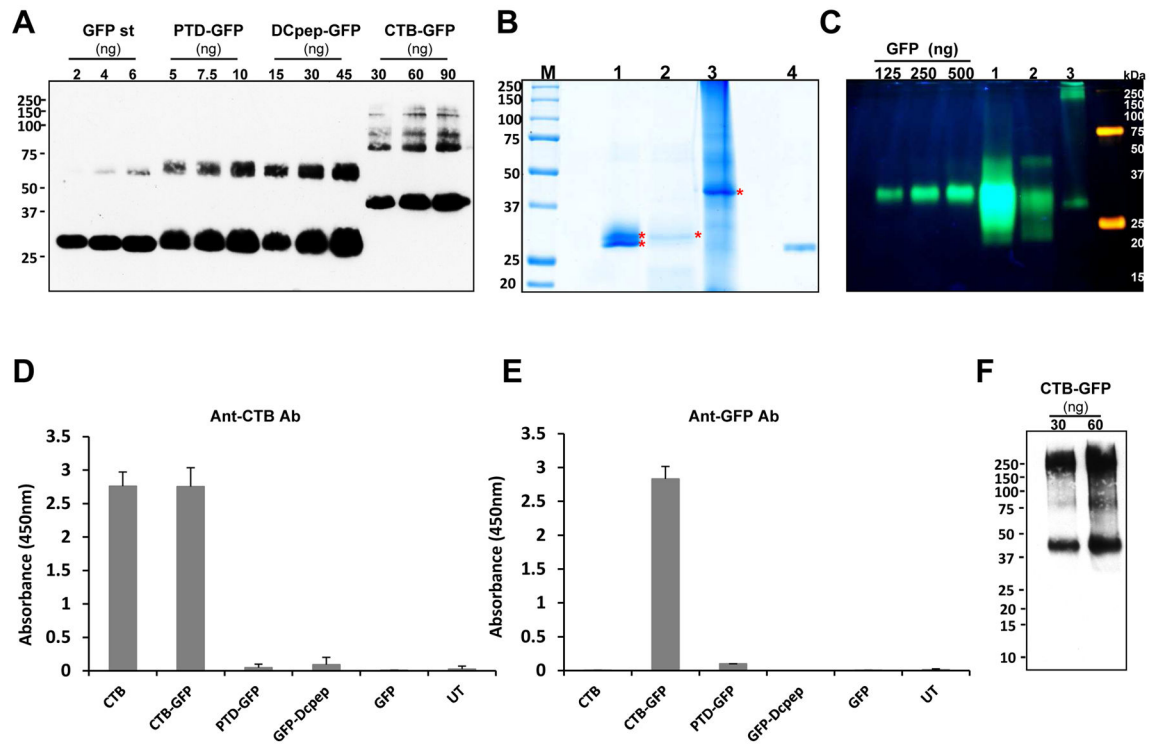
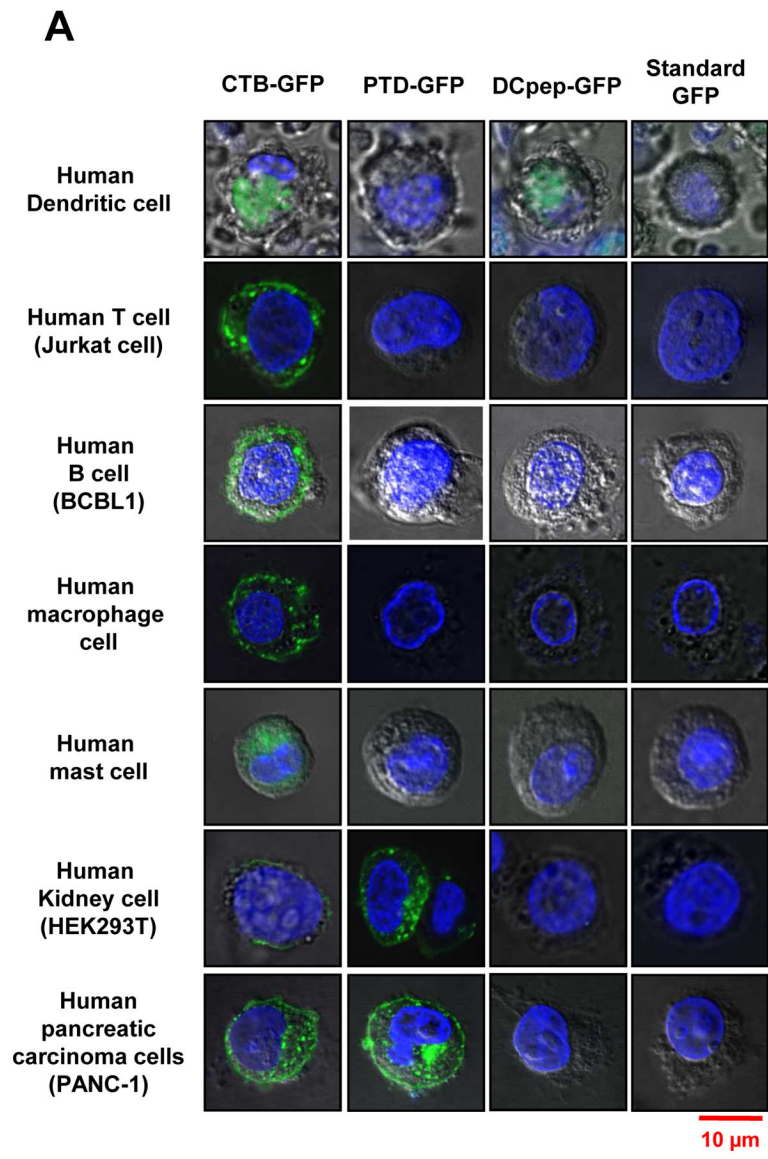


Fig. 4. Characterization of purified GFP fused proteins

(A) Quantification of purified GFP fused proteins, and coomassie staining and fluorescence image. Densitometric assay with western blot image was done with known amount of GFP standard protein to quantify the purified tag-fused GFP proteins. Purified proteins were run on SDS- PAGE and immunoprobed with anti-GFP antibody. Loading amounts were indicated as shown. Purity was calculated as a percentage of the amount detected on the immunoblot assay to total loading amount. (B) Coomassie staining of purified GFP tagged proteins. M, protein molecular weight marker; lane 1, PTD-GFP (10 μ L, 2.37 μ g); lane 2, Dcpep-GFP (40 μ L, 3.12 μ g), lane 3, CTB-GFP (10 μ L, 32.8 μ g), and lane 4, GFP (400 ng). (C) Non-denaturing SDS-PAGE of purified GFP fusion proteins in order to determine GFP fluorescence. Lane 1 (PTD-GFP 10 μ L, 9.17 μ g TSP loading), lane 2 (DCpep-GFP 15 μ L, 4.6 μ g TSP loading) and lane 3 (CTB-GFP 20 μ L, 33 μ g TSP loading). (D and E) The purified GFP-tagged proteins were examined for their binding affinity to GM1 receptor. Anti-CTB (D) and anti-GFP (E) antibody were used to detect the interaction between GM1 and the GFP fusion proteins. The protein amounts used for the assay are as follows. CTB, 10 pg; CTB-GFP, 1.25 ng; PTD-GFP 10ng; DCpep-GFP 10ng; GFP, 10ng and UT, untransformed wild type total proteins, 100ng. (F) Non-denaturing Tris-tricine PAGE of purified CTB-GFP to determine pentameric structure. Pentameric structure of purified CTB-GFP was immunoprobed using anti-CTB antibody (1 in 10,000). Loading amounts of CTB-GFP are indicated as in the figure.



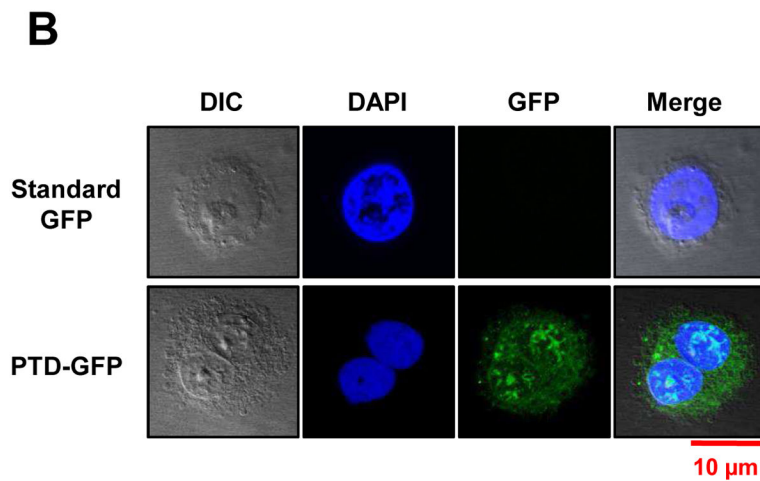


Fig. 5. Uptake of GFP fused with different tags by human immune and non-immune cells
 (A) Translocation of purified GFP fusion proteins in human cell lines. 2×10^4 cells of cultured human dendritic cell (DC), B cell, T cell and mast cells were incubated with purified GFP fusion: CTB-GFP (8.8 μ g/100 μ l PBS), PTD-GFP (13 μ g/100 μ l PBS), DCpep-GFP (1.3 μ g/100 μ l PBS) and commercial standard GFP (2.0 μ g/100 μ l PBS) respectively, at 37°C for 1 hour. After PBS washing, B, T and mast cell pellets were stained with 1:3000 diluted DAPI and fixed with 2% paraformaldehyde. Then the cells were sealed on slides and examined by confocal microscopy. Live DCs were stained with 1:3000 diluted Hoechst and directly detected under the confocal microscope. For 293T, pancreatic cells (PANC-1 and HPDE) and macrophage cells, eight-well chamber slides were used for cell culture at 37°C for overnight. After incubated with purified CTB-GFP (8.8 μ g/100 μ l PBS), PTD-GFP (13 μ g/100 μ l PBS), DCpep-GFP (1.3 μ g/100 μ l PBS) and commercial standard GFP (2.0 μ g/100 μ l PBS) respectively, at 37 °C for 1 hour, washed in PBS and stained nuclei with 1:3000 DAPI. (B) Nuclear localization of PTD-GFP in human pancreatic ductal epithelial cells (HPDE). Green fluorescence shows GFP expression; blue fluorescence shows cell nuclei labeling with DAPI. The images were observed at 100x magnification. Scale bar represent 10 μ m. All images studies have been analyzed in triplicate.

Table 1
Uptake efficiency of purified GFP fusion proteins in human cell lines

The relative delivery efficiency of GFP to human cell lines by three different tags was compared by counting the number of cells showing GFP signals under confocal microscope at 100x magnification. A total of 15–20 images were observed for each cell line. All cell lines were examined in triplicate.

	CTB-GFP	PTD-GFP	DCpep-GFP
Human Dendritic cell	70.4 % (19/27)	0% (0/12)	83% (10/12)
Human T cell	91.7 % (11/12)	0% (0/18)	0% (0/13)
Human B cell	87.5 % (14/16)	0% (0/14)	0% (0/10)
Human macrophage cell	91.7 % (11/12)	0 % (0/12)	0 % (0/12)
Human mast cell	91.7 % (11/12)	0 % (0/12)	0% (0/11)
Human Kidney cell	83.3 % (12/13)	83.3 % (10/12)	0% (0/10)
Human pancreatic cells	89.5 % (17/19)	81.2% (9/11)	0% (0/12)